MICROBIAL GENOMICS

RESEARCH ARTICLE
Brown *et al.*, *Microbial Genomics* 2026;12:001731
DOI 10.1099/mgen.0.001731

MICROBIOLOGY SOCIETY
OPEN DATA OPEN ACCESS

The effects of bacteriophage cocktail treatment on healthy gut microbiota: an *in vitro* human colon model study

Teagan L. Brown[1], Duncan Y.K. Ng[1], George M. Savva[1], Claire K.A. Elek[1,2], James A.D. Docherty[1,2], Ryan Cook[1], Rebecca Ansorge[1], Andrea Telatin[1], Elizabeth Kutter[3] and Evelien M. Adriaenssens[1,*]

Abstract

The human gut microbiome is a complex community that plays an important role in health, where perturbations can result in dysbiosis and disease. Bacteriophages (phages) can provide treatment for bacterial gastrointestinal disease, and commercial preparations such as the Intesti bacteriophage cocktail can be taken orally to target bacterial pathogens. However, interactions between these phages and the native gut microbiota are understudied. To investigate the impact of phage treatment, we used simulated gut models seeded with healthy donor microbiota from three individuals, sequenced the DNA and analysed the bacterial and viral portions from samples obtained over time. Each donor had a unique bacterial composition that diverged with time. When comparing phage-treated to control samples, we observed that *Escherichia coli* abundance accounted for the largest portion of bacterial community variance and was more associated with the controls. The lower abundance in phage-treated samples may have resulted from the lytic action of phages from the cocktail. Additionally, our analyses of the viral portion revealed a phage bloom exclusive to phage-treated samples. A highly abundant phage in this bloom was matched with the Intesti bacteriophage cocktail, showed similarity to *Enterobacteria* phage phi92 and provided evidence of productive infection within the model. While we did observe fluctuations in relative abundance of additional viral sequences in the presence of the phage cocktail, these changes were often transient. Furthermore, we detected only slight differences from typical members of the virome and low numbers of active prophages. Our experiments suggest that the phage cocktail had minimal interruption to the native gut microbiota within the model.

Impact Statement

Bacteriophages are increasingly investigated and tested for their efficacy in treating infections and are a key component in the fight against antimicrobial-resistant bacterial infections. Because of their specificity, it has become almost a dogma to state that they do not alter the gut microbiome. We have now tested this in an *in vitro* study using a commercially available cocktail and real human faecal microbiota. We show minimal effects on the composition of the healthy microbiota with an individual-specific effect on *Escherichia coli* caused by productive infection of one phage in the cocktail.

DATA AVAILABILITY

The raw reads of all shotgun metagenomics experiments are available from the European Nucleotide Archive under Project accession number PRJEB96854. Accession numbers of the individual runs are listed in Table S1. A curated database of the assembled viral operational taxonomic units can be accessed on FigShare at the following link: https://doi.org/10.6084/m9.figshare.31016773.

Received 30 January 2026; Accepted 04 May 2026; Published 21 May 2026
Author affiliations: [1]Quadram Institute Bioscience, Norwich Research Park, Norwich, UK; [2]University of East Anglia, School of Biological Sciences, Norwich, UK; [3]Phagebiotics Research Foundation, Olympia, USA.
***Correspondence:** Evelien M. Adriaenssens, evelien.adriaenssens@quadram.ac.uk
Keywords: bacteriophage cocktail; gut microbiota; shotgun metagenomics; virome.
Abbreviations: CDS, coding sequences; dbRDA, distance-based redundancy analysis; DTRs, direct terminal repeats; ENA, European Nucleotide Archive; IGV, Integrative Genomics Viewer; NCBI, National Center for Biotechnology Information; NMDS, non-metric multi-dimensional scaling; UViG, uncultivated viral genomes; vOTUs, viral operational taxonomic units.
All supporting data, code and protocols have been provided within the article or through supplementary data files. Eleven supplementary tables are available with the online version of this article.

INTRODUCTION

The gut microbiome plays an essential role in human health and often is an indicator of disease development and progression [1]. Members of the phyla *Bacteroidota* and *Bacillota* dominate the bacterial portion of a healthy human adult gut, and studies report *Bacteroidaceae*, *Clostridiaceae*, *Prevotellaceae*, *Ruminococcaceae*, *Lachnospiraceae*, *Oscillospiraceae*, *Bifidobacteriaceae*, *Lactobacillaceae* and the *Enterobacteriaceae* as the most abundant families [2–4]. Enterotypes, and more recently enterosignatures, have been used to describe the bacterial community at the genus level, with the *Bacteroides* (western) and *Prevotella* (non-western) enterosignatures core to a healthy adult microbiome [5–7].

The viral portion of the gut microbiome (virome), largely represented by bacteriophages (phages), is thought to play a significant role in the community by shaping the bacteria and represents vast, often undescribed diversity [8, 9]. The development of improved viral detection tools [10–12], human gut virome-specific databases [9, 13–16] and viral mining pipelines [17, 18] have resulted in higher recovery of viruses from metagenomic datasets, and ongoing efforts continue to taxonomically classify the diversity [19]. A longitudinal study has shown that adult gut viromes are individualized and temporally stable but are often dominated by dsDNA phages from the order *Crassvirales*, which show widespread distribution across multiple datasets [13, 20–22], as well as *Microviridae* (ssDNA) phages [23].

To investigate the dynamics of the gut microbiome in response to a range of stresses and conditions, *in vitro* model systems have been invaluable. These systems have been used to simulate bacterial dynamics in response to chemical and diet changes by static batch fermentation culture [24, 25], continuous culture systems with mono or multi-stage compartments [26–28] or the use of microfluidic organ-on-chip models [29, 30]. While acute changes to the gut microbiota composition can occur due to several factors, including the physical environment, nutrition, infection, medication and genetics, chronic or large shifts in the community can result in dysbiosis and disease states [31–33]. Diarrhoea, dysentery, enterocolitis and dysbacteriosis are common complaints of the gastrointestinal tract, often associated with bacterial pathogens [34]. The use of antibiotics to treat diseases caused by these pathogens can have short-term (e.g. diarrhoea, *Clostridioides difficile* infection) but also profound and long-lasting effects on the composition of the gut microbiota [35–38].

An alternative treatment for bacterial infectious disease is the use of phages (single or in cocktails), which were first investigated over 100 years ago in the treatment of dysentery [39, 40]. In recent years, phage therapy has gained in popularity, having been effectively used (alone or as adjunctive therapy) to remedy many human infections including chronic rhinosinusitis [41], urinary tract infection [42–44], lung and respiratory infection [45–48], endocarditis [49], cranial osteomyelitis [50] and traumatic injury [51] involving one or multiple bacterial species.

The integration of phages into *in vitro* gut models has provided greater insight into host–phage interactions and the dynamics of the gut microbiota. An *Escherichia coli* phage [52] and a four-phage cocktail against *C. difficile* [53] were tested in batch fermentation experiments using faecal slurries spiked with host bacteria. Batch models comprised of multiple compartments have been seeded with a seven-strain 'ileal microbiota' mix and tested against *E. coli* [54] and *Listeria monocytogenes* [55] phages. Best representing gut conditions, continuous culture multi-stage systems containing faecal slurries have been utilized to explore *Klebsiella* [56] and *Salmonella* [57] lysis by phages. While some studies also rigorously assessed prophylactic and remedial use [53, 57], the reports suggested that phages successfully reduced pathogens without impacting the gut microbiota within the system [52–57].

One commercially available phage preparation for treating gastrointestinal disease is the Intesti bacteriophage cocktail manufactured by the Eliava Institute (Tbilisi, Georgia), where phage therapy has been in use since the 1920s [58–60]. This formulation has successfully been used prophylactically and at the onset of disease and contains in excess of 20 lytic phages for 7 pathogenic genera: *Enterococcus*, *Escherichia*, *Proteus*, *Pseudomonas*, *Salmonella*, *Shigella* and *Staphylococcus* [58, 61]. Despite its extensive use, safety and efficacy, little is known about how the phage cocktail affects the healthy gut microbiome. In this study, we assessed changes in the adult gut microbiota following Intesti bacteriophage cocktail administration using a human colon model system and shotgun metagenomic sequencing.

METHODS

Phage cocktail

The Intesti bacteriophage cocktail was manufactured by the George Eliava Institute of Bacteriophages, Microbiology and Virology in Georgia. The cocktail was purchased over-the-counter at the Eliava Institute, Tbilisi, Georgia, for use in these experiments (batch M2-901).

Media and reaction vessel conditions

Our experiments were conducted using an *in vitro* batch-culture fermentation colon model as described previously [24]. We used 100-ml reusable glass vessels with a working volume of 50 ml, which were autoclaved prior to experiments. Nutritive media

used in the reaction vessel was composed of 2 g l^{-1} of each peptone water, sodium bicarbonate ($NaHCO_3$) and yeast extract, 0.5 g l^{-1} of bile salts and cysteine-HCl, 0.1 g l^{-1} of sodium chloride, 0.04 g l^{-1} of each di-potassium hydrogen phosphate (K_2HP0_4) and potassium di-hydrogen phosphate (KH_2P0_4), 0.02 g l^{-1} haemin, 0.01 g l^{-1} of each magnesium sulphate heptahydrate ($MgS0_4.7H_20$) and calcium chloride dihydrate ($CaCl_2.2H_20$), 2 ml of Tween 80 and 10 µl of vitamin K1. During the experiments, the temperature was maintained at 37 °C with a circulating water jacket, and anaerobic conditions were held constant with nitrogen gas bubbling through the media. The pH was held at 6.6 to 7.0 with the addition of 1 M NaOH and HCl solutions using Fermac 260 control units (Electrolab, UK). A magnetic stirrer at ~60 r.p.m. ensured proper mixing of the faecal slurry in the vessels and the maintenance of anaerobic conditions and pH throughout the experiment.

Ethical approval

Three donor faecal samples were obtained from participants recruited onto the Quadram Institute Bioscience Colon Model study. Stool sample collection for use in *in vitro* fermentation experiments was approved by the Quadram Institute Bioscience Human Research Governance Committee (IFR01/2015) and the Westminster Research Ethics Committee (15/LO/2169) and is registered (http://www.clinicaltrials.gov registration NCT02653001). Informed consent of all subjects was obtained.

Faecal samples and sampling

Participants providing the faecal samples were over the age of 18, working or living within 10 miles of the Norwich Research Park (coordinates 52.620889, 1.218744); had normal bowel habits (regular defecation between three times a day to three times a week, with a Bristol stool type of 3–5); and were not diagnosed with chronic gastrointestinal health problems (such as irritable bowel syndrome, coeliac or inflammatory bowel diseases). At the time of collection, participants completed a survey which confirmed they had not taken antibiotics or probiotics in the previous 4 weeks, had no gastrointestinal complaints or surgery requiring anaesthetics within the last 72 h nor were they currently pregnant or breastfeeding.

For our study here, three healthy adult donor faecal samples were collected fresh on the morning of the experiment and transported to the institute in triple-protected containers at room temperature for immediate processing. Each donor faecal sample was seeded into two reaction vessels, one for the Intesti bacteriophage cocktail treatment and the other serving as a control. Prior to seeding the reaction vessels, the donor faecal samples were separately homogenized as follows. Ten grams of the faecal sample was combined in a stomacher bag with 90 ml of sterile PBS at pH 7.4 (PBS, 2.7 mM KCl, 10 mM Na_2HPO_4 and 1 mM KH_2PO_4). The sample was homogenized with a stomacher 400 (Seward, UK) for 45 s at 230 r.p.m. Five millilitres of the resulting slurry was used to seed 44 ml of nutritive media for both the phage-treated and control vessels. One millilitre of Intesti bacteriophage cocktail was added to the phage-treated vessel 15 min after seeding and 1 ml of PBS to the control vessels. Five hundred microlitre samples of the faecal slurries were taken in triplicate from both vessels immediately after the addition of the phage, then again 6 and 24 h later. The samples were stored at −80 °C until further processing.

DNA extraction and metagenomic sequencing

DNA extraction was performed using two 500 µl aliquots (1 ml total) of the faecal slurries taken at each time point. DNA from 10 ml of the Intesti bacteriophage cocktail was extracted to serve as a positive control, whereas a mock community (suspension of *E. coli* W1485 bacterial cell culture and two lab-isolated phages classified as *Jedunavirus* and *Chivirus*) was extracted to detect any kit contamination or artefacts. Prior to the extraction, bacteriophages and cellular material were co-precipitated by the addition of polyethylene glycol (PEG_{8000}) and sodium chloride at final concentrations of 8% and 0.3 M, respectively. The precipitation was incubated at 4 °C overnight before being centrifuged at 13,000 ***g*** for 10 min. The supernatant was removed, and the pellet was re-suspended in 750 µl of PowerBead solution (kit supplied), and 60 µl of solution C1 (QIAGEN DNeasy PowerLyzer PowerSoil Kit) was added. The contents were then subjected to bead beating homogenization at 4,000 r.p.m. for 15 s, using a FastPrep-24 classic (MP Biomedicals, USA). The DNA extraction was conducted according to the manufacturer's instructions (QIAGEN DNeasy PowerLyzer PowerSoil Kit). The DNA was eluted in 100 µl solution C6 (kit supplied) and was stored at −80 °C prior to sequencing. The DNA samples were sent to Novogene (Cambridge, UK) for Nextera XT DNA library preparation and shotgun metagenomic sequencing, using the Illumina NovaSeq 6000 system with an S4 flow cell and 150-bp paired-end reads.

Bioinformatics and data analysis

Reads obtained from sequencing were checked for Illumina adapters, the human contaminant and phiX174 sequencing standard reads were removed and the minimum PHRED quality was set to 20 using fastp [62]. The reads obtained from this study were deposited into the European Nucleotide Archive (ENA) under the study PRJEB96854. For individual sample ENA accessions and associated metadata, see Table S1 (available in the online Supplementary Material). The quality reads were taxonomically profiled with MetaPhlAn3 (v3.0) [63] and Kraken2 (v2.1.0) [64] using the k2_pluspf_20210517 database. For more accurate species abundance values, the Kraken2 taxonomic data were re-estimated using Bracken (v2.6.0) [65]. Genera and species relative abundance data were initially visualized in Phantasus (v1.15.4) [66], and further analysis of the bracken taxonomic data was handled within R (v4.1.2). To compare the profiles obtained and patterns between samples, a heatmap of the relative species (top

500) was generated, using pheatmap (v1.0.12) and viridis (v0.6.4) colour palette packages, where values were scaled by row, and the rows were clustered by Euclidean distance and Ward linkage. Further, a barplot of the top six genera (by maximum percentage) was visualized to show abundance changes across all samples. Alpha and beta diversities, analysis of the variance and redundancy were calculated on the species abundance table using the vegan (v2.5–7) [67] and microbiome (v1.20.0) packages, where the counts were rarefied to the sample with the lowest number of bacterial reads (1.6×10^6; 2B3). The ordination for beta diversity was based on non-metric multi-dimensional scaling (NMDS) of a Bray–Curtis dissimilarity matrix, generated by the metaMDS function within the vegan package. Analysis of the community data variance between control and phage-treated samples was computed using the varpart function within the vegan package (on the Bray–Curtis dissimilarity), where phage treatment, donor and time were explanatory variables. A distance matrix and principal coordinates were the basis for a distance-based redundancy analysis (dbRDA) ordination, which was constrained by phage treatment.

To best recover viruses from the samples, we utilized an assembly approach where the high-quality reads were assembled with MEGAHIT (v1.1.3) [68] using default k-mer lengths of 21, 29, 39, 59, 79, 99, 119 and 141. Viral and phage sequences were predicted from these assembled contigs with VIBRANT (v1.2.1) [10] using the default settings with a minimum sequence length of 1 Kb and VirSorter2 (v2.2.3) [12] with a minimum sequence length of 1.5 Kb and the default dsDNA/ssDNA database. VIBRANT and VirSorter2 predicted viral sequence files (for each sample) were labelled and concatenated with SeqFu (v1.9.1) [69]. This resulted in a collection of uncultivated viral genomes (UViG) predicted for all the samples, which could be prepared for further analyses using Anvi'o (v7.1) [70, 71]. The individual UViG files (.fasta) were concatenated with SeqFu and dereplicated twice, firstly using CD-HIT-EST (v4.8.1) [72] at 95% identity (-c 0.95) with a 99% sequence alignment (-aS 0.99) and then using rapid genome clustering in CheckV (v1.0.1) [73] with an average nucleotide identity of 95% and an alignment fraction of 85%, to approximate species-level clusters for dsDNA prokaryotic viruses of the class *Caudoviricetes*, as defined by the International Committee on Taxonomy of Viruses [74]. The dereplicated dataset consisted of species-level viral operational taxonomic units (vOTUs), which were each represented by their largest UViG. Only the vOTUs greater than 4.5 Kb were retained, resulting in the final contig/vOTU database. Coverage and detection of the vOTUs from the contig database were established through read mapping of the donor and phage cocktail read libraries with Bowtie2 (v2.4.1) [75] end-to-end mapping (default settings and penalties) in conjunction with SAMtools (v1.12) [76]. Within Anvi'o (v7.1), the resulting BAM files were individually profiled against the contig database, which was functionally annotated using the NCBI (National Center for Biotechnology Information) COGs database (COG20) [77] and had tRNAs identified [78]. The profiles were then merged to observe patterns in the viral species present. In case of contamination, any vOTUs showing mapping with the mock community were excluded from further analysis. The taxonomic diversity of the phage sequences found in the contig database was assessed using a gene-sharing network with vConTACT2 [79], annotated using the INPHARED pipeline [80]. Briefly, the contigs in the vOTU database were annotated using PHANOTATE with the Pharokka pipeline (v1.1.0) [81]. The annotated files were transformed into the input format for vConTACT2 using the script single_GenBank_to_vConTACT_inputs (https://github.com/RyanCook94/Random-Perl-Scripts/blob/main/single_GenBank_to_vConTACT_inputs.pl). The annotated contig .faa file and the INPHARED database file 2Nov2022_vConTACT2_proteins.faa were concatenated and used as input for the --raw-proteins in vConTACT2, as were the gene to genome mapping files for input as the --proteins-fp. vConTACT2 was run without an internal database, using DIAMOND [82] for protein clustering and ClusterONE [83] for genome clustering. The resulting network was visualized with Cytoscape (v3.9.1) [84] and annotated with the INPHARED database annotation tables dated on 2 November 2022.

Where comparative genomics between our phage and database phages was required, we annotated individual genomes (as above using PHANOTATE in the Pharokka pipeline v1.1.0) before gene clusters were analysed using Clinker (v.0.0.23) [85]. Individual read mapping across one genome was viewed by Integrative Genomics Viewer (IGV) (v2.6.1) [86]. Input files for IGV were generated with SAM tools (v1.12) and BamToCov (v2.7.0) [87].

To link potential phage sequences with their predicted bacterial hosts, we used iPHoP (v1.2.0) [88]. Phage lifestyle was predicted as a part of CheckV 'prophage' analysis and by BACPHLIP (v0.9.3) [89]. Potential prophage activity was estimated with PropagAtE (v1.0.0) [90] using MEGAHIT-assembled contigs and VIBRANT-generated prophage coordinates.

RESULTS

To simulate the human gut system and gut microbiota, we used an *in vitro* batch-culture fermentation colon model seeded with faecal samples from three healthy donors. For assessment of the microbial changes, each donor had an untreated control and a phage cocktail-treated vessel, and these faecal slurries were sampled over time at phage addition (0 h), 6 h and 24 h. The total microbial DNA was extracted and sequenced, and we obtained 21–35 million quality reads per sample (Table S1).

Composition of the microbiome

Across the three donor samples, we detected over 100 distinct bacterial genera and viral species with scantily detected archaeal and no fungal signatures. At the species level, little overlap in gut microbial composition was observed between individuals (Fig. 1a). While the exact composition was unique, several bacterial genera, which are typical members of the human gut microbiota,

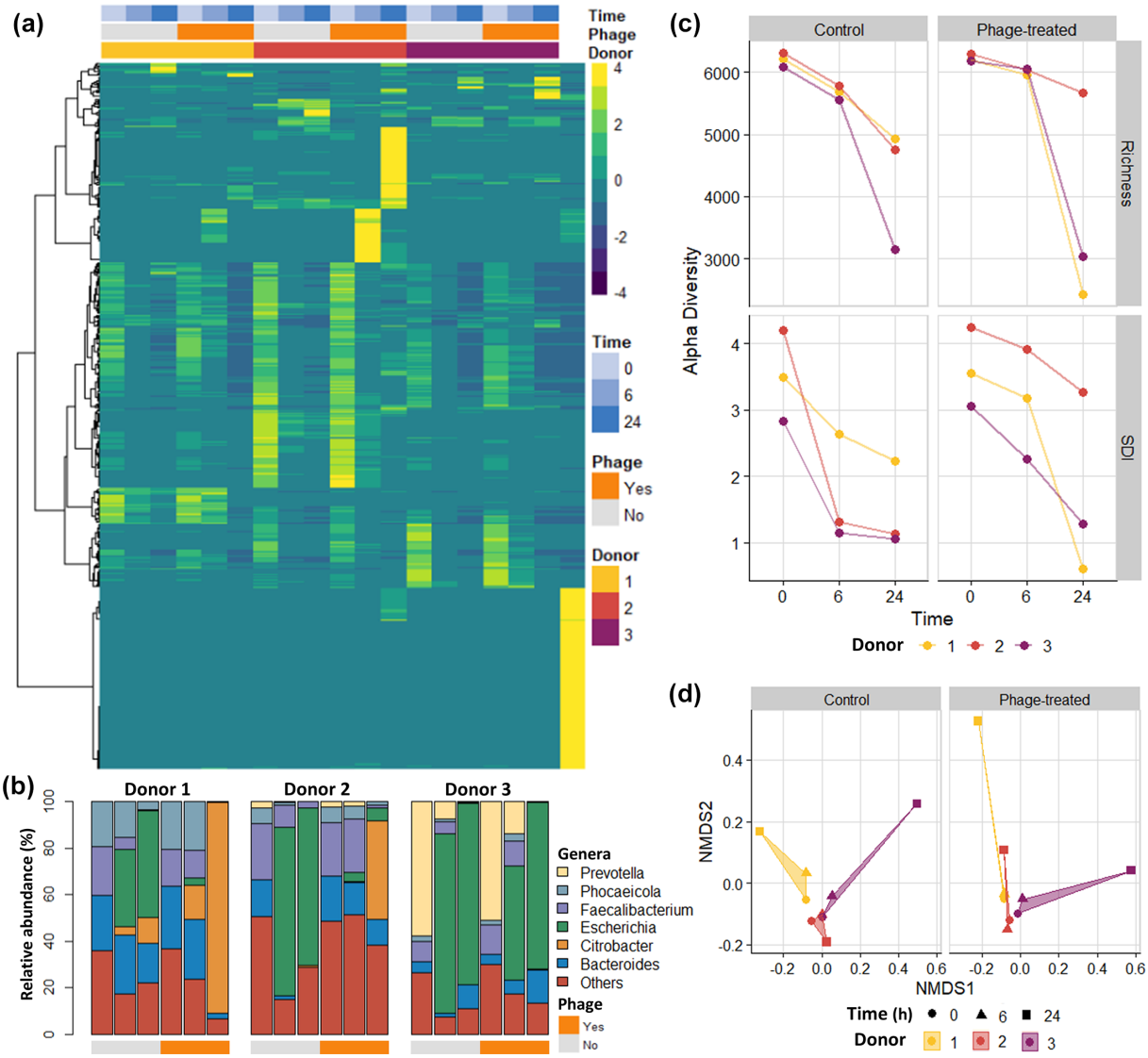

Fig. 1. Microbial diversity of samples. (a) Heatmap of the relative abundance of the top 500 species as determined by Bracken. The columns represent the samples and the phage cocktail (rightmost column). The rows indicate the identified viral or bacterial species, and these were hierarchically clustered by Euclidean distance and Ward linkage. The relative abundance was scaled by row. (b) Genus relative abundances across samples. Samples are grouped by donor, ordered by time (0, 6 and 24 h), and are divided by treatment, where control and phage treatment are coloured in grey and orange, respectively. (c) Alpha diversity indices of the samples (richness and Shannon diversity index) separated by phage treatment. Points represent individual samples across time points. (d) Sample beta diversity and NMDS plots according to phage treatment. The stress value for the plot is 0.26.

including *Bacillus*, *Bacteroides*, *Eubacterium*, *Faecalibacterium, Lactobacillus* and *Phocaeicola*, were detected in all three donors. *Bacteroides* and *Faecalibacterium* were ubiquitous, detected in the top six most abundant genera of both the control and phage-treated samples (Fig. 1b), whereas genera such as *Bifidobacterium*, *Prevotella* and *Streptococcus* were more abundant in specific donors (donor 1, 3 and 2, respectively), and their abundance decreased over time.

Initially, donor one derived samples contained similar proportions of *Bacteroides*, *Faecalibacterium* and *Phocaeicola* (Fig. 1b), with the remaining portion composed of *Ruminococcus*, *Bifidobacterium* and many other genera. However, the samples derived from donor 2 had more *Faecalibacterium* present with less *Bacteroides*, and all other genera were below 10% relative abundance each. *Prevotella* dominated samples derived from donor 3, with a relative abundance over 50% (Fig. 1b). These initial compositions altered markedly over the course of the experiment (Fig. 1b). Opportunistic and adaptive bacteria belonging to the genera *Escherichia*, *Klebsiella*, *Proteus*, *Salmonella*, *Serratia* and *Veillonella* had the highest abundance after the initial time point in one or more donor-derived samples. This was particularly evident for *Escherichia* and *Citrobacter* (Fig. 1b). As the microbiota adapted to the condition of the model gut system, we observed reductions in the alpha diversity (Fig. 1c). The richness and Shannon

diversity index were the highest initially then decreased over the course of the experiment, a trend seen in both the control- and phage-treated samples (Fig. 1c). Likewise, the beta diversity at first was similar across samples before diverging over time (Fig. 1d).

These analyses revealed changes in bacterial composition not only with phage treatment but also by individual donor and time. Permutational multivariate ANOVA with sequential tests with adonis2 for donor, time and phage were statistically significant for all at *P*-values of 0.001, 0.001 and 0.042, respectively. To estimate how much of the community variation could be attributed to each variable, we used Bray–Curtis dissimilarity in conjunction with variation partitioning. Changes over time contributed 31.5% of the variance in the composition data, and donors represented 14.2%, whereas phage treatment only contributed 2.8% of the variance (adjusted R^2 values). Next, we used dbRDA to identify the main changes in bacterial relative abundance according to phage treatment (Fig. 2a). The bacterial species most impacted was *E. coli*, which was more closely associated with the controls. In contrast, we observed that *Citrobacter koseri* and *Faecalibacterium prausnitzii* were more abundant in phage-treated samples, whereas *Prevotella copri* showed similar relative abundances, irrespective of the phage treatment (Fig. 2a). The relative abundance of these species differed by time and donor (Fig. 2b–e). *E. coli* abundance increased after the initial timepoint, was detected in all donor-derived samples and was reduced in phage-treated samples compared to the controls (Fig. 2b). Similarly, *C. koseri* abundance increased over time; however, the species was more prevalent in the phage-treated samples of two donors, especially those derived from donor 1 (Fig. 2d). Over the course of the experiment, *P. copri* abundance decreased in donor 3 control and phage-treated samples (Fig. 2c). *F. prausnitzii* relative abundance also decreased over time but was found in all three donor samples (Fig. 2e). While full interactions and population dynamics in the system were not known and our sample size did not permit statistical testing, our observations suggest that *E. coli* abundance was reduced by the lytic action of phages from the cocktail. Lysis due to the phage cocktail phages also could have left nutrients for other bacteria, such as *F. prausnitzii* to grow within the model.

Phage cocktail phages have the potential to actively replicate in the healthy gut

We next looked at the phage portion of the microbiome to investigate whether phages from the cocktail were actively replicating in our model system, thereby influencing the bacterial composition. This analysis was complicated by the observation that the read profilers were not able to distinguish well between different phage signatures, especially at the species level. We, therefore, used the gold-standard pipeline of assembly, phage identification, vOTU clustering and read mapping for analysis (see the 'Methods' section; as previously described [91]). Across all libraries excluding the mock community, we generated a virus contig database of 5,306 vOTUs, where each vOTU was represented by the largest contig or UViG, which were classified by CheckV as complete (66/5,306), high-quality (103/5,306), medium-quality (182/5,306), low-quality (2,189/5,306), and the remainder were not-determined (2,766) (Table S2; vOTU database available on FigShare). Read mapping of these vOTUs and visualization with Anvi'o allowed us to discern which vOTUs were present in the phage cocktail. These analyses revealed that only 166 vOTUs recruited reads from the phage cocktail library using a detection limit of 0.25 (i.e. minimum 25% of the contig length covered by reads) and minimum average coverage over 1 (Fig. 3). It is important to note here that we chose this approach because the phage cocktail itself had a low number of phages per millilitre and direct assembly yielded only a low number of high-quality UViGs.

The percentage of mapped reads from each sample recruited to the phage cocktail vOTUs ranged from 76% (donor 2 samples at 6 h) to 0.1% (as seen in all controls at time zero), with an average depth of coverage from 1,292× to almost zero (Table S3). The phage cocktail vOTUs ranged in size from 4.5 to 147 kb, with approximately half over 10 kb in length. Direct terminal repeats (DTRs) were identified in 5 sequences, which were marked as complete by CheckV and of the remaining, 6 were classified as high-quality, 6 as medium-quality and 149 as low-quality, with the low-quality vOTUs likely representing short genome fragments rather than being individual phages (Table S2). We discovered that 75 of the 166 vOTUs detected were exclusively found in the cocktail, and conversely, 24 were detected in phage-treated samples as well as control samples, indicating that a subset of phages in the phage cocktail are related to natural members of the gut microbiota. Of the 67 vOTUs found only in phage-treated vessels, the majority (46/67) were detected in all phage-treated vessels, suggesting detection irrespective of their replication within the model, whereas others found in 1 (18/67) or 2 (3/67) donor-derived samples may be reliant on replication for detection.

To gain insight into the taxonomic diversity of the vOTUs found in the phage cocktail, we constructed a gene-sharing network using vConTACT2, where each phage or vOTU contig is a node connected with an edge if they share a significant number of genes. The network revealed that vOTUs detected in the phage cocktail were more closely associated with reference sequences as opposed to donor-derived viral sequences detected in our study (Fig. 4). Further investigation of the 166 phage cocktail vOTUs showed that 60 were assigned viral clusters, and of these, only 14 also contained representatives from the INPHARED database. An additional 5 vOTUs were found to overlap clusters, while the number of singletons and outliers totalled 101 (Tables S2 and S4). Considering the clustering, read mapping patterns and completeness, our sequencing here produced 11 unique phage genomes, which were marked (by CheckV analysis) as complete with DTRs or high-quality genomes from the phage cocktail (Table 1). We also observed the presence of partial phage genomes, which pertained to six unique viral clusters containing database representatives and numerous other contigs that were singletons or outliers in the

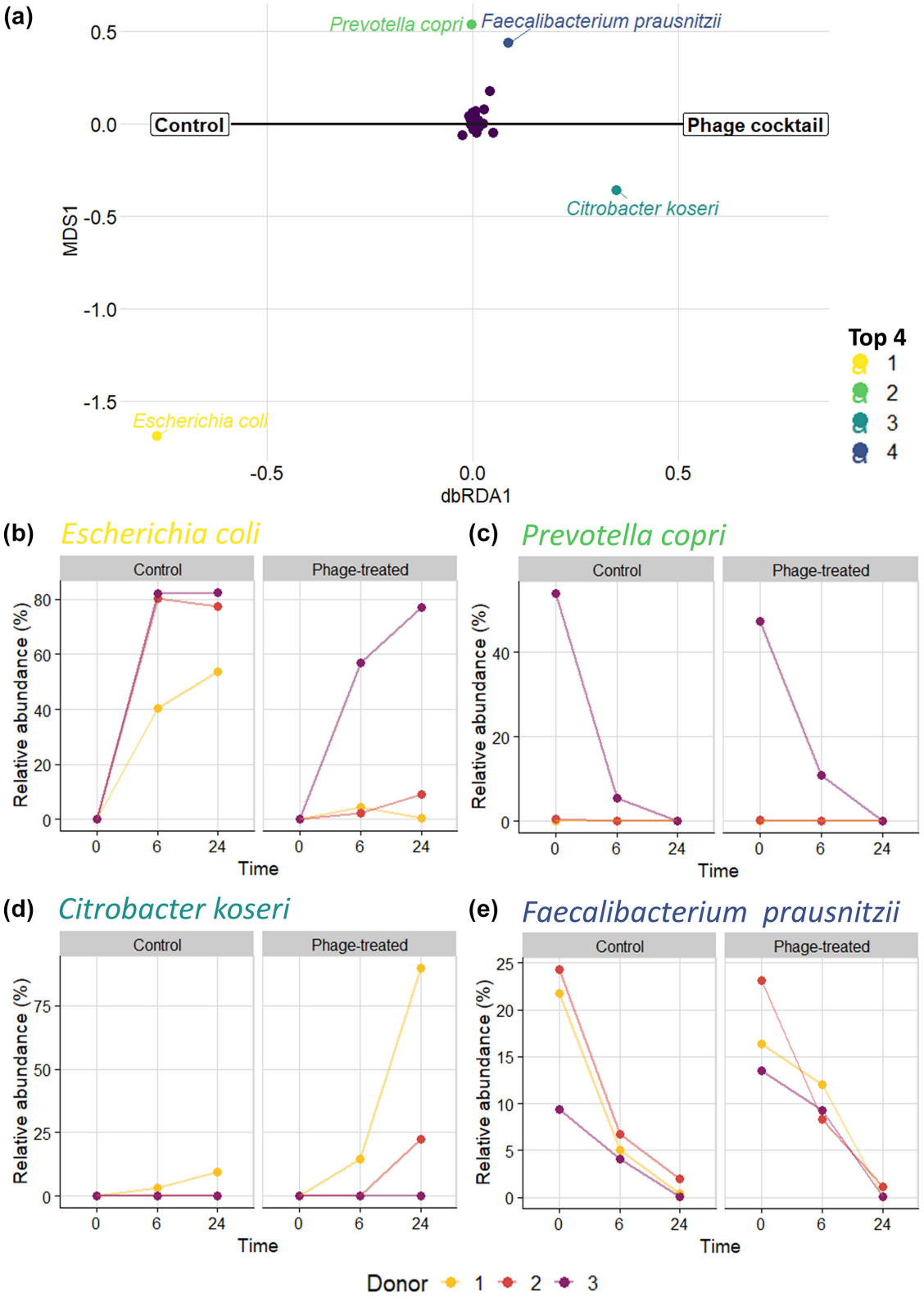

Fig. 2. Bacterial community composition dynamics separated by phage treatment. A dbRDA plot (a) constrained by phage treatment (*X*-axis), showing the top four most impacted bacterial species. Their location relative to the centrepoint (*X*=0) indicates association with control (left) or phage-treated (right) samples. Plots of the relative abundance of the top four species (b–e), separated by phage treatment, illustrate variation over time and by donor.

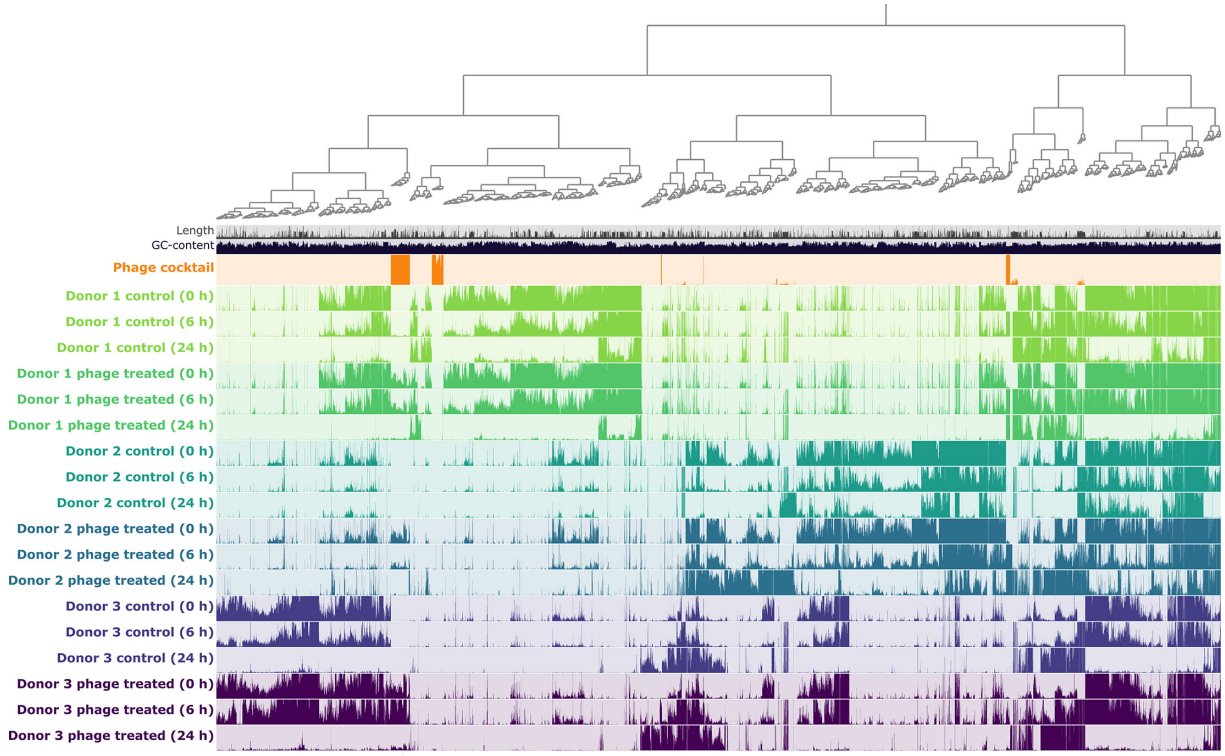

Fig. 3. Differential abundance of the virus contig database. Tracks represent sample sequence libraries, and each column represents a vOTU or split (contigs were split into multiple sections if the length was longer than 20 kb). The height of the bar within the tracks depicts the mean coverage of vOTUs or splits to a maximum of 10× coverage. The dendrogram shows clustering according to sequence composition and differential coverage (Euclidean distance and Ward linkage). Figure created using Anvi'o.

gene-sharing network and of low quality (Tables S2 and S4). The phage cocktail contained sequences from diverse virus taxa, clustering with known members from *Dhillonvirus, Justusliebigvirus, Nankokuvirus, Phietavirus* and *Saphexavirus* genera (Fig. 4 and Table 1). Of note, we also identified a high-quality UViG, which clustered with 29 unclassified *Streptococcus* phages, a genus or host not reported to be targeted by the Intesti bacteriophage cocktail. Further diversity was discovered in shorter vOTUs clustered with known larger viral sequences from genera such as *Astrithrvirus*, *Berlinvirus*, *Chivirus*, *Peduovirus* and *Tequintavirus* (Fig. 4, Tables S2 and S4), as well as outlier and singleton BLASTN similarity (at species level demarcation >95% identity over 99% query) with *Asteriusvirus*, *Kayvirus*, *Felixounavirus*, *Kochikohdavirus*, *Mosigvirus* and *Tequatrovirus*.

We compared our clustered UViGs to previously defined phage clusters by Zschach *et al.* [61] to explore the diversity of phages within the Intesti bacteriophage cocktail and discovered that only 4 (out of 11; 36%) of our UViGs group with the 18 previously described phage clusters (Table 1) and an additional 2 were clustered with incomplete vOTUs from our data (*Berlinvirus* and *Vequintavirus*). While not clustered, some vOTUs representative of the *Chivirus*, *Drexlerviridae* and *Kayvirus* genera were identified in both studies. Our sequencing here revealed increased diversity from the phage cocktail, as we identified UViGs which cluster with known *Phietavirus*, *Novosibvirus* and an unclassified *Enterococcus* phage, as well as partial vOTUs from *Peduovirus* and *Kochikohdavirus*. Furthermore, host prediction indicated that these phages could target members of *Enterococcus*, *Escherichia*, *Proteus*, *Pseudomonas*, *Salmonella*, *Staphylococcus* and *Streptococcus* and, therefore, could impact the microbiota in our gut model (Table 1).

As phages may influence the bacteria, we looked for phages undergoing active infection in our model, i.e. phage cocktail vOTUs with increased read mapping at 6 and 24 h, over 10× coverage increase and with reads mapped to at least 80% of the vOTU length (Anvi'o detection limit of 0.8). We identified a subset of 32 vOTUs with greater than 10× difference in average coverage compared with the control coverage. However, these often were not representative of full genomes, not clustered with known INPHARED database phages, nor had a predicted host (Tables S3 and S5). Their elevated coverage indicated growth in the model system, but their impact on the community was unknown.

Considering only the complete and high-quality vOTUs identified in our study (Table 1), six were also detected at over 10× coverage in selected donor-derived samples and were elevated compared to the control (Table S3). In donor 3-derived samples,

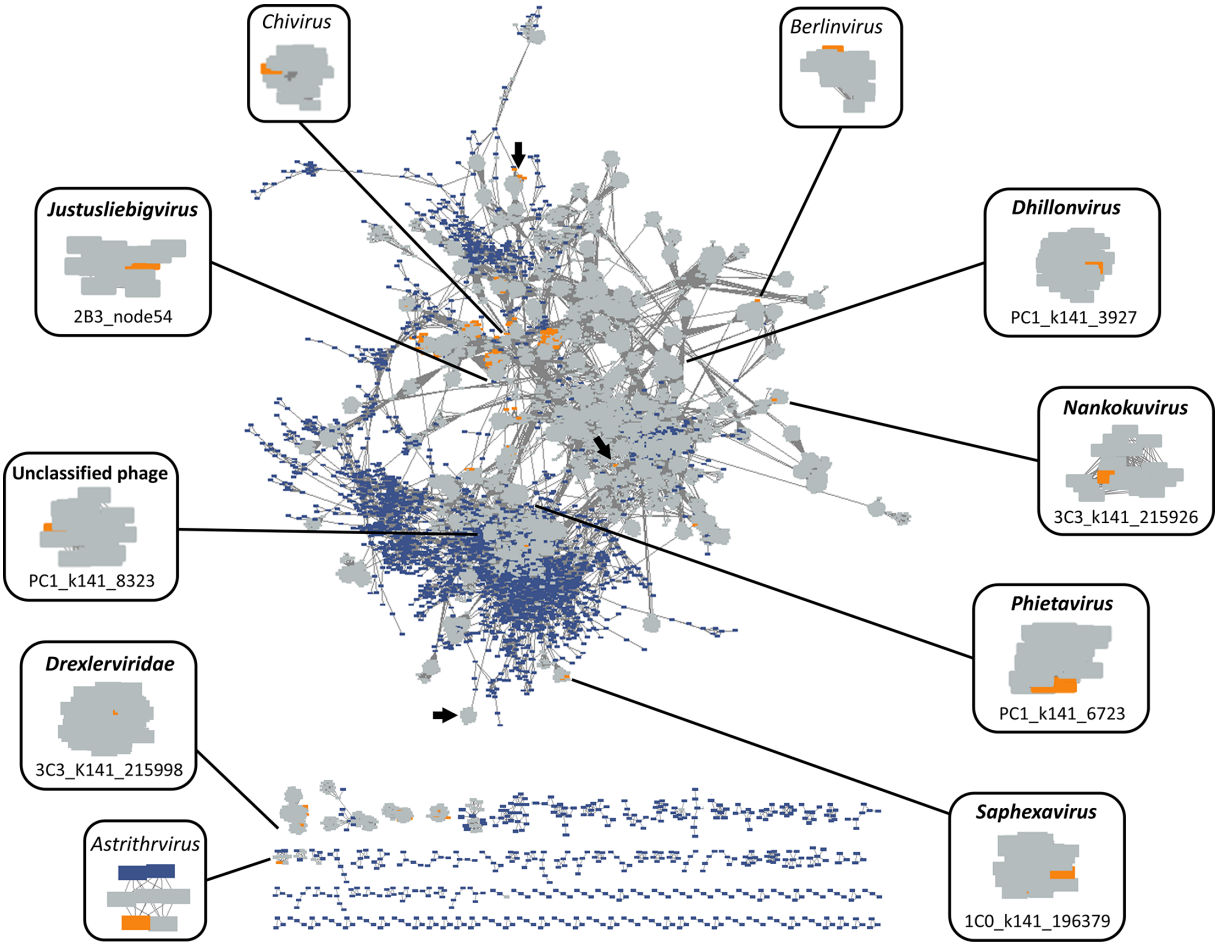

Fig. 4. Predicted vOTU gene-sharing network. Known phages from the INPHARED reference database are represented as coloured grey rectangles, all contig database predicted vOTUs across our dataset are marked in blue and vOTUs detected in the phage cocktail are marked in orange. Annotated are virus genera or families and individual phage which cluster at that classification. Complete or high-quality sequences that overlap clusters are marked with arrows.

we discovered that the *Novosibvirus*, *Nankokuvirus*, *Saphexavirus*, *Drexlerviridae* (family) and unclassified *Enterococcus* phages had the highest read mapping (<100 times) at 6 h, demonstrating the phages' response to fluctuations in their host bacteria over the course of the experiment. We uncovered the largest increase in average coverage across all phage cocktail vOTUs from the high-quality 147 kb *Justusliebigvirus* phage (Table 1), which had closest sequence similarity and gene structure to *Enterobacteria* phage phi92 with 247 coding sequences (CDS) and 14 tRNAs (Fig. 5a). This phage, we labelled as '*Justusliebigvirus* bloom phage', was overrepresented in donor 2-derived samples at 6 and 24 h with an average coverage of over 23,000× and 1,700×, respectively, as well as ~80× coverage in the donor 3-derived sample at 24 h (Fig. 5b). We found this phage at a low average coverage (1.45×) in cocktail and other donor-derived samples (Fig. 5b); thus, replication must have occurred within the vessel, and this likely depended on the growth of *E. coli*.

Also present with high coverage at the same time point and vessel as the *Justusliebigvirus* bloom phage were several shorter vOTUs. While these vOTUs did not cluster in the vConTACT2 network, they shared similarity to multiple members of the genus *Tequatrovirus* by BLASTN similarity at species level demarcation, and we hypothesize that these contigs together could be equivalent to a predicted complete genome, which did not assemble. These two phages together (*Justusliebigvirus* bloom phage and unknown *Tequatrovirus*) account for ~85% of the viral reads in the donor 2-derived 6 h sample.

Impacts of the phage cocktail on the gut microbiota are often transient

Given the replication of the *Justusliebigvirus* bloom phage and the apparent lysis of *E. coli* within the donor 2 phage-treated vessel, we searched for subsequent effects by scanning for elevated vOTUs at 24 h. From the entire phage contig database, we uncovered 12 high-quality vOTUs that had their highest average coverage at this time point, 10 of which were donor 2-specific, and three

Table 1. Intesti bacteriophage cocktail sequences

Contig ID	Contig length (bp)	Sequence quality; completeness (%)*	Taxonomy and viral cluster data†	Previous sequencing data (accession; cluster and size)‡	Detection§	Predicted host genus (% confidence)¶
3C3_k141_215395	103,658	Complete (100; DTR)	Overlaps two clusters; *Novosibvirus*		PC; three phage-treated	*Proteus* (97.5)
3C3_k141_215926	87,887	Complete (100; DTR)	*Nankokuvirus* cluster (20 viruses)	*Nankokuvirus* (KC862301; D3=87,828 bp)	PC; three phage-treated	*Pseudomonas* (100)
1C0_k141_196379	57,076	Complete (100; DTR)	*Saphexavirus* cluster (33 viruses)	*Saphexavirus* (KJ094032; D7=58,193 bp)	PC; controls; three phage-treated	
3C3_k141_215998	46,178	Complete (100; DTR)	*Drexlerviridae* cluster (62 viruses)		PC; three phage-treated	*Escherichia* (98.4)
PC1_k141_7426	43,359	Complete (100; DTR)	Overlaps two clusters; unclassified *Pseudomonas* virus		PC only	*Pseudomonas* (99.7)
2B3_node54	147,148	High-quality (97.35)	*Justusliebigvirus* cluster (27 viruses)	*Justusliebigvirus* (FR775895; D5=150,530 bp)	PC; two phage-treated	
PC1_k141_4175	46,712	High-quality (98.6)	Outlier		PC only	*Salmonella* (99.4)
PC1_k141_3927	42,446	High-quality (94.92)	*Dhillonvirus* cluster (67 viruses)	*Dhillonvirus* (KM233151; D16=46,882 bp)	PC only	*Escherichia* (99.1)
PC1_k141_6723	42,405	High-quality (98.66)	*Phietavirus* cluster (20 viruses)		PC only	*Staphylococcus* (100)
PC1_k141_2544	40,824	High-quality (96.6)	Overlaps two clusters; unclassified *Enterococcus* virus		PC; three phage-treated	*Enterococcus* (97.8)
PC1_k141_8323	32,503	High-quality (100)	Unclassified *Streptococcus* phage; cluster 29 phages		PC only	*Streptococcus* (100)

*Completeness as determined by CheckV analyses.
†vConTACT2 cluster data. Phage clusters here also contained INPHARED database phages, and clusters which overlap show manually assigned taxonomy based on the closest relative nucleotide sequence similarity.
‡Zschach *et al*. [61] sequencing cluster data, which were updated to show the latest taxonomy. Accession represents the closest relative reference, and the cluster is per notation from the original work.
§Detection was determined from the read-mapping data within Anvi'o. PC is the phage cocktail, the control and the number of donor-derived phage-treated samples in which the sequence was found is indicated.
¶Host as predicted by IPHoP, shown here are genera where the confidence values >95%.

clustered within our vConTACT2 network (Tables S6 and S7). A total of eight vOTUs were only detected at 24 h, including one (2B5_k141_64032) that clustered with unclassified *Escherichia* phage vB_EcoM-613R2, a prophage of *E. coli* [92], and was marked by BACPHLIP as temperate (Table S6). Also clustered with *Rauchvirus* prophages was another vOTU (2B5_k141_55335), which was detected initially in both the control and phage-treated samples, and then again at 24 h, but only in the phage-treated vessel with over a hundred times average coverage. These two vOTUs likely would have relied on the stress of *E. coli* and *Bordetella*, respectively, which occurred prior to the 24 h sample. The final vOTU to cluster (with three unclassified phages), 2B5_k141_91452, was marked as lytic but was only present at the final time point in excess of 170 times coverage in the phage-treated vessel but minimally in the control. The known phages in the cluster all have unique hosts, and a host was not predicted for the vOTU with iPHoP, but it is likely that the host was able to make use of byproducts produced from other bacteria or was non-fastidious. The impact of this vOTU on the community and those also unclassified was unknown.

Next, we investigated whether typical members of the gut virome were altered in the phage cocktail-treated vessels by observing changes in average coverage of vOTUs clustered with members of the *Crassvirales* order and the *Microviridae* family. From our vConTACT2 network, we identified three *Crassvirales* and two *Microviridae* vOTUs, which were marked as lytic by BACPHLIP (Table S8). The three *Crassvirales* vOTUs were representative of three families, *Crevaviridae*, *Intestiviridae* and *Steigviridae*,

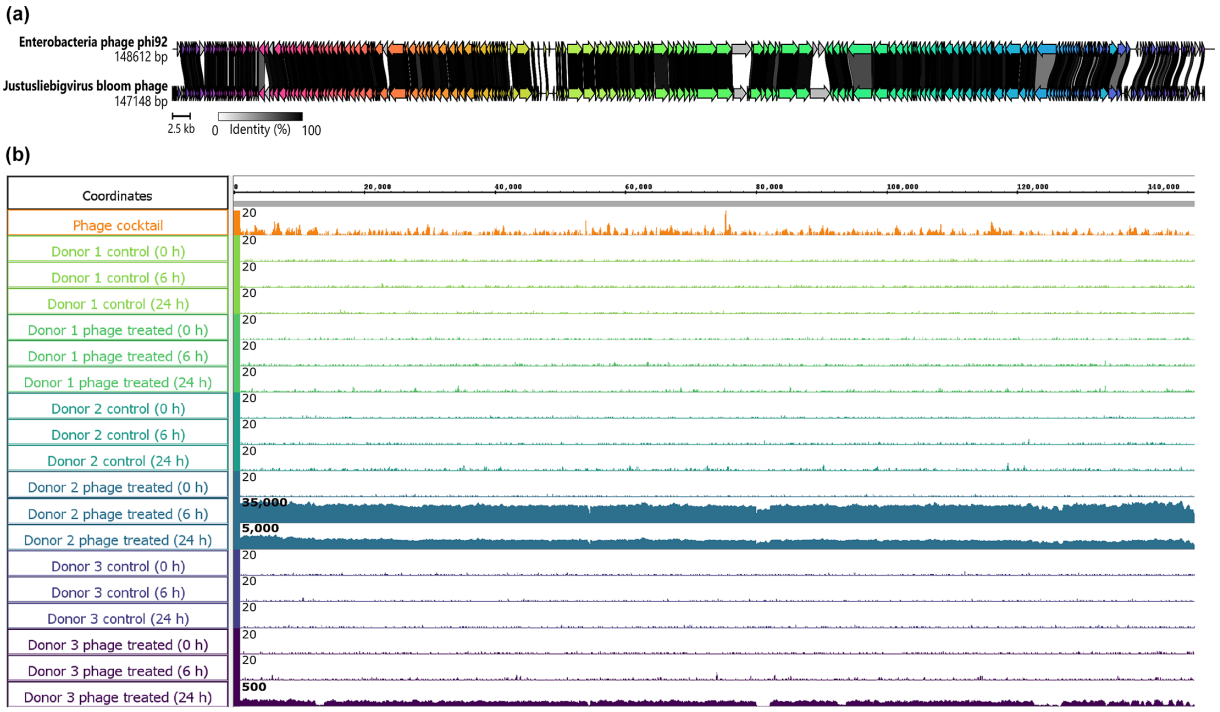

Fig. 5. Genome representation of the phage present in the phage bloom and read mapping across the donor-derived samples. Represented is the genome structure and comparative genomics between the *Justusliebigvirus* bloom phage and *Enterobacteria* phage phi92 (a), where arrows indicate predicted genes, colour shows homologous genes and the links indicate nucleotide similarity between the coding sequences. Read mapping of the genome with donor-derived sample libraries (b). Each track represents a sample, and the height of the bars represents the reads mapped at that location, with the maximum of the scale noted at the upper left corner.

and were specific to donor 3-, 2- and 1-derived samples respectively, within the control and phage-treated vessels. The *Crevaviridae* vOTU (3A0_k141_46950) in the phage-treated vessel had approximately four times higher average coverage than the control at 6 h; however, at 24 h, the level was equivalent to the control. Although shorter than a predicted genome, we uncovered that the *Intestiviridae* vOTU (2B5_k141_39930) had a 100-fold increase in coverage compared with the control at 24 h. Conversely, the *Steigviridae* (1A0_k141_190349) vOTU showed similar patterns of coverage across 6 and 24 h. We discovered that the two *Microviridae* vOTUs were exclusive to donor 2 control and phage-treated samples. One vOTU (2A0_k141_222313) was maintained across timepoints, whereas the other (2B0_k141_198670) showed the highest coverage at the initial timepoint, but both were concordant with the control (Tables S7 and S8).

Our analysis of the bacterial community composition suggested that there were increased levels of *C. koseri* and *F. prausnitzii* signatures detected in the presence of the phage cocktail. In an effort to link these bacteria with specific vOTUs, we searched for those clustering with known phages infecting these specific hosts and subsequently alterations in their coverage. There were no *Citrobacter* phages clustered with the vOTUs in our database; however, guided by the Kraken2 results, we discovered the top six vOTUs (by average coverage) in the donor 1 phage-treated vessel at 24 h and had BLASTN similarity (at species demarcation) to *C. koseri* (Tables S7 and S9). With thousands of times coverage, at levels ten times greater than the control, two vOTUs (1A5_k141_68270_0; 2B5_k141_36022) indicated stress of the bacteria and bacterial defence systems. One was a 1-kb fragment that contained a portal protein and may indicate release of a cryptic prophage or one that did not assemble, and the other had a type I-F CRISPR/Cas system (contained within an 86-kb sequence) with two short CRISPR loci that may have prevented phage predation of the bacteria. While the remaining vOTUs were marked as bacterial (false positives) or were detected in the mock community (possible contaminants), one (1A5_k141_30475), a 300 kb vOTU, contained a 50-kb predicted complete prophage sequence (as determined by checkV) at levels tenfold greater than the control. Further analysis showed that mock community reads mapped to bacterial genes outside of the predicted prophage region and moreover indicated that there were multiple prophages at this time point, which may have contributed to the levels of *Citrobacter* detected within the vessel. We identified six high-quality, complete vOTUs in the dataset that clustered with *Faecalibacterium* phages, but their coverage changes were small and could not be linked to bacterial abundance (Tables S7 and S10). A result also reflected in the vOTUs, which were predicted to have *F. prausnitzii* as a host.

One potential side effect of phage cocktail treatment could be the induction of prophages from the native bacteria present in the donor sample. To investigate whether the temperate phages identified in our gut model were actively replicating, the PropagAtE prediction

was used, where differences in read mapping to the bacterial chromosome and the prophage coordinates inferred replication status. With this tool, the number of induced prophages found in all samples was low, and there were no apparent differences between the phage-treated and control samples (Table S11). However, individual phage–bacteria interactions by induced prophages, such as those hypothesized in donor 2-derived samples (as detailed above) and other episomal prophage interactions, could have been impacting the bacterial community over time.

DISCUSSION

An ideal phage cocktail is one that contains strictly lytic phages that lyse pathogenic bacteria contributing to disease, while leaving the resident microflora unaffected. Given the complex microbial structure of the human gut and its integral role in health [1], effective and specific lytic phages are particularly advantageous. Phage preparations, such as the Intesti bacteriophage cocktail, are available for purchase to treat common gastrointestinal complaints and, when taken orally, are exposed to the resident gut microbiota. However, the impact on these communities is understudied. Our study here described changes in both the bacterial and viral communities from three healthy individuals in the presence of the Intesti bacteriophage cocktail, using a simulated gut model. Despite the many complex dynamics and interplays, our results suggest that fluctuations in bacteria and viruses associated with the phage cocktail had minimal interruption to the native gut microbiota within the model.

The gut models linked with all three donors were colonized by the typical members of human gut microbiota. We detected the presence of *Bacteroides* and *Faecalibacterium* in all donor samples, whereas genera, such as *Bifidobacterium*, *Prevotella* and *Streptococcus*, were donor-specific and often transient across time points, which is consistent with community dynamics in the gut ecosystem [93]. Our profiling and the community composition at the initial time point indicated the donors had healthy gut microbiome enterosignatures, where two microbiomes were *Bacteroides* (ES-Bact) and the other was *Prevotella* (ES-Prev) centric. Each donor had a unique bacterial community at the species level and the diversity decreased over the course of the experiment. This was reflected in the calculated diversity indices and increased abundance of non-fastidious bacteria such as *Escherichia*. Given the static nature of our experimental model and once-supplied media within the system, this decrease in diversity was expected and was a limitation of the study.

The bacterial community composition altered over the course of the experiment. Our analysis using time, donor and phage treatment as explanatory variables and Bray–Curtis distance revealed that the largest impact on the community variance was time, whereas phage treatment contributed under 3%. When comparing phage treatment to controls, the most impacted species was *E. coli*, which was less abundant in phage-treated samples at 6 and 24 h. Although our study is not powered for statistical testing, we observed a reduction of *E. coli* signatures in all phage-treated vessels and detected *E. coli* phages within the experimental system (as discussed below), which potentially impacted the bacterial community. While the full pathogenicity and impact of the strains remain unknown, a decreased abundance of *E. coli* may be beneficial in a treatment setting to reduce disease symptoms and restore gut eubiosis.

Our sequencing effort here captured as yet uncultured phage isolates, as compared with the previously reported cocktail diversity, and indicated that the Intesti bacteriophage cocktail is composed of numerous phages from various taxonomic genera. Previous work by Zschach *et al.* [61] reported the cocktail to contain 22 phage clusters, which were derived by propagating phages from the preparation. Our direct sequencing approach, creation of a contig database, followed by read mapping and vOTU clustering, revealed both taxonomically similar and diverse phages within the phage cocktail at the genus level and potentially novel taxonomic diversity. The presence of an unclassified *Streptococcus* phage with an average coverage of 17× over the entire sequence from the phage cocktail library was unexpected, as it is not a host reported to be targeted by the Intesti bacteriophage cocktail. This phage was not found to replicate in phage-treated vessels and may have been introduced to the cocktail prior to our study.

Productive infection of the Intesti bacteriophage cocktail-derived phages was occurring within our gut model. We observed the *Justusliebigvirus* bloom phage, which was overrepresented in donor 2-derived samples with average coverage in excess of 1,000 times. Its high sequence identity to the *E. coli*-infecting phage phi92 makes it likely that the bloom phage also infects *E. coli* or a related strain. Similarly, most members of the genus *Tequatrovirus* are known to lyse *E. coli* or *Shigella* strains, and we, therefore, speculate that this minor bloom phage also infects *E. coli*. In parallel, we observed a decrease in *E. coli* signatures, not just in the sample undergoing the active phage bloom but also in other phage-treated donors and time points. From this, we have good evidence to conclude that the Intesti bacteriophage cocktail influences the *Escherichia* populations in the gut. However, we currently do not have enough sequence data to ascertain what strains of *E. coli* are affected and whether these are considered commensals in healthy adults or whether they are opportunistic pathogens that could lead to disease development.

The microbiota in the system adapted to changed conditions. Following the phage bloom in the donor 2 phage-treated vessel, there was an increase in high-quality vOTUs at 24 h. The majority of these were specific to the donor 2 vessel at that time point and include both lytic and temperate vOTU (as predicted by BACPHLIP). A vOTU that clustered with *Rauchvirus* prophage was detected initially and again at 24 h, indicating the potential for native donor phages to modulate gut bacteria.

Phage treatment appeared to minimally affect the native microbiota. Typical members of the gut virome, *Crassvirales* and *Microvidae* viruses, were detected in our dataset, but each vOTU was limited to one donor's sample rather than being ubiquitous. We observed that vOTUs were often present across all time points and concordant in both control and phage-treated samples, indicating their stability

and persistence in the donor microbiota. Our analysis showed an increase of *C. koseri* and *F. prausnitzii* in phage-treated vessels; however, their levels could not be linked to vOTU abundance changes. The vOTUs we did detect indicated stress of the *Citrobacter* population, increased bacterial defence systems and potential prophage induction. Given that the bacterial data were derived from read profiling, it is possible that the increase in *C. koseri* signatures was linked to prophages, which were misidentified as bacterial. The lytic action of the phage cocktail could also have allowed these bacteria to flourish. Although the *Justusliebigvirus* phage bloom observation was the most pronounced change in the system, additional phage/host interactions were likely occurring here without great disturbance. Our gut model and analysis form the basis to investigate changes to bacterial and viral communities in the presence of phage treatment and has the potential to be utilized with other phage cocktails or formulations. However, our small study would have benefited from more donor samples and replication to better define statistical differences between phage treatment and controls. Furthermore, deeper sequencing and strain-level analyses of metagenome-assembled bacterial genomes would be advantageous in disentangling the intricate interactions and dynamics between the healthy bacteria and phage communities in the gut.

CONCLUSIONS

The commercially available Intesti bacteriophage cocktail preparation may be taken orally to target common bacterial infections of the human gastrointestinal tract, but little is known about how the phages interact with the native gut microbiota. Our simulated gut model was seeded with microbiota consistent with healthy-donor enterosignatures, and our sequencing method enabled us to observe bacterial and viral community changes. Each donor had a unique bacterial composition that altered over time. When comparing phage-treated and control samples, *E. coli* had the largest difference in relative abundance and was more closely associated with the controls. This observation suggests lytic action from the phages in the cocktail, such as the *Justusliebigvirus* bloom phage. Changes to the microbiota and impact of phage cocktail treatment were often transient, where we detected minimal changes to typical members of the virome and active prophages in the system. While the full impact of the phage cocktail on the gut microbiota is not known, these initial experiments suggest that the Intesti bacteriophage cocktail minimally interrupted the native gut microbiota in the model.

Funding information
T.L.B., A.T., R.A. and E.M.A. gratefully acknowledge funding by the Biotechnology and Biological Sciences Research Council (BBSRC) Institute Strategic Programme Gut Microbes and Health BB/R012490/1 and its constituent projects BBS/E/F/000PR10353 and BBS/E/F/000PR10356. E.M.A. is currently funded by the BBSRC Institute Strategic Programme Food Microbiome and Health BB/X011054/1 and its constituent projects BBS/E/QU/230001B and BBS/E/QU/230001D and the BBSRC Institute Strategic Programme Microbes and Food Safety BB/X011011/1 and its constituent projects BBS/E/QU/230002A, BBS/E/QU/230002B and BBS/E/QU/230002C. R.C. and E.M.A. are funded through the Biotechnology and Biological Sciences Research Council (BBSRC) grant Bacteriophages in Gut Health BB/W015706/1. G.M.S. was supported by the BBSRC Core Capability Grant BB/CCG2260/1. J.A.D.D. was supported by the UKRI Biotechnology and Biological Sciences Research Council (BBSRC) Doctoral Training Partnership BB/M011216/1. C.K.A.E. was supported by the Medical Research Council (MRC) as part of the Doctoral Antimicrobial Research Training (DART) MRC iCASE Programme MR/R015937/1. A.T. and R.A. were supported by the Quadram Institute Bioscience BBSRC funded Core Capability Grant BB/CCG1860/1.

Acknowledgements
The authors would like to acknowledge Oliver Charity for useful discussions regarding data analysis. The authors acknowledge the use of the QIB Colon Model Facility and thank the manager, Lee Kellingray, for facilitating and advising on this project.

Conflicts of interest
The authors declare that there are no conflicts of interest.

References

1. Manor O, Dai CL, Kornilov SA, Smith B, Price ND, *et al*. Health and disease markers correlate with gut microbiome composition across thousands of people. *Nat Commun* 2020;11:5206.
2. Lloyd-Price J, Abu-Ali G, Huttenhower C. The healthy human microbiome. *Genome Med* 2016;8:51.
3. Mirzaei MK, Maurice CF. Ménage à trois in the human gut: interactions between host, bacteria and phages. *Nat Rev Microbiol* 2017;15:397–408.
4. Rinninella E, Raoul P, Cintoni M, Franceschi F, Miggiano GAD, *et al*. What is the healthy gut microbiota composition? A changing ecosystem across age, environment, diet, and diseases. *Microorganisms* 2019;7:14.
5. Arumugam M, Raes J, Pelletier E, Le Paslier D, Yamada T, *et al*. Enterotypes of the human gut microbiome. *Nature* 2011;473:174–180.
6. Costea PI, Hildebrand F, Arumugam M, Bäckhed F, Blaser MJ, *et al*. Enterotypes in the landscape of gut microbial community composition. *Nat Microbiol* 2018;3:8–16.
7. Frioux C, Ansorge R, Özkurt E, Ghassemi Nedjad C, Fritscher J, *et al*. Enterosignatures define common bacterial guilds in the human gut microbiome. *Cell Host Microbe* 2023;31:1111–1125.
8. Shkoporov AN, Hill C. Bacteriophages of the human gut: the "known unknown" of the microbiome. *Cell Host Microbe* 2019;25:195–209.
9. Gregory AC, Zablocki O, Zayed AA, Howell A, Bolduc B, *et al*. The gut virome database reveals age-dependent patterns of virome diversity in the human gut. *Cell Host Microbe* 2020;28:724–740.
10. Kieft K, Zhou Z, Anantharaman K. VIBRANT: automated recovery, annotation and curation of microbial viruses, and evaluation of viral community function from genomic sequences. *Microbiome* 2020;8:90.
11. Ren J, Song K, Deng C, Ahlgren NA, Fuhrman JA, *et al*. Identifying viruses from metagenomic data using deep learning. *Quant Biol* 2020;8:64–77.
12. Guo J, Bolduc B, Zayed AA, Varsani A, Dominguez-Huerta G, *et al*. VirSorter2: a multi-classifier, expert-guided approach to detect diverse DNA and RNA viruses. *Microbiome* 2021;9:37.
13. Camarillo-Guerrero LF, Almeida A, Rangel-Pineros G, Finn RD, Lawley TD. Massive expansion of human gut bacteriophage diversity. *Cell* 2021;184:1098–1109.
14. Van Espen L, Bak EG, Beller L, Close L, Deboutte W, *et al*. A previously undescribed highly prevalent phage identified in a Danish enteric virome catalog. *mSystems* 2021;6:e0038221.

15. Nayfach S, Páez-Espino D, Call L, Low SJ, Sberro H, *et al*. Metagenomic compendium of 189,680 DNA viruses from the human gut microbiome. *Nat Microbiol* 2021;6:960–970.
16. Tisza MJ, Buck CB. A catalog of tens of thousands of viruses from human metagenomes reveals hidden associations with chronic diseases. *Proc Natl Acad Sci USA* 2021;118:e2023202118.
17. Pandolfo M, Telatin A, Lazzari G, Adriaenssens EM, Vitulo N. MetaPhage: an automated pipeline for analyzing, annotating, and classifying bacteriophages in metagenomics sequencing data. *mSystems* 2022;7:e0074122.
18. Pinto Y, Chakraborty M, Jain N, Bhatt AS. Phage-inclusive profiling of human gut microbiomes with Phanta. *Nat Biotechnol* 2024;42:651–662.
19. Turner D, Shkoporov AN, Lood C, Millard AD, Dutilh BE, *et al*. Abolishment of morphology-based taxa and change to binomial species names: 2022 taxonomy update of the ICTV bacterial viruses subcommittee. *Arch Virol* 2023;168:74.
20. Edwards RA, Vega AA, Norman HM, Ohaeri M, Levi K, *et al*. Global phylogeography and ancient evolution of the widespread human gut virus crAssphage. *Nat Microbiol* 2019;4:1727–1736.
21. Gulyaeva A, Garmaeva S, Ruigrok RAAA, Wang D, Riksen NP, *et al*. Discovery, diversity, and functional associations of crAss-like phages in human gut metagenomes from four Dutch cohorts. *Cell Rep* 2022;38:110204.
22. Ramos-Barbero MD, Gómez-Gómez C, Sala-Comorera L, Rodríguez-Rubio L, Morales-Cortes S, *et al*. Characterization of crAss-like phage isolates highlights *Crassvirales* genetic heterogeneity and worldwide distribution. *Nat Commun* 2023;14:4295.
23. Shkoporov AN, Clooney AG, Sutton TDS, Ryan FJ, Daly KM, *et al*. The human gut virome is highly diverse, stable, and individual specific. *Cell Host Microbe* 2019;26:527–541.
24. Day-Walsh P, Shehata E, Saha S, Savva GM, Nemeckova B, *et al*. The use of an *in-vitro* batch fermentation (human colon) model for investigating mechanisms of TMA production from choline, L-carnitine and related precursors by the human gut microbiota. *Eur J Nutr* 2021;60:3987–3999.
25. Pérez-Burillo S, Molino S, Navajas-Porras B, Valverde-Moya ÁJ, Hinojosa-Nogueira D, *et al*. An *in vitro* batch fermentation protocol for studying the contribution of food to gut microbiota composition and functionality. *Nat Protoc* 2021;16:3186–3209.
26. Firrman J, Liu L, Mahalak K, Tanes C, Bittinger K, *et al*. Comparative analysis of the gut microbiota cultured *in vitro* using a single colon versus a 3-stage colon experimental design. *Appl Microbiol Biotechnol* 2021;105:3353–3367.
27. Salgaço MK, Perina NP, Tomé TM, Mosquera EMB, Lazarini T, *et al*. Probiotic infant cereal improves children's gut microbiota: insights using the Simulator of Human Intestinal Microbial Ecosystem (SHIME®). *Food Res Int* 2021;143:110292.
28. Davis Birch WA, Moura IB, Ewin DJ, Wilcox MH, Buckley AM, *et al*. MiGut: a scalable *in vitro* platform for simulating the human gut microbiome—development, validation and simulation of antibiotic-induced dysbiosis. *Microb Biotechnol* 2023;16:1312–1324.
29. Jalili-Firoozinezhad S, Gazzaniga FS, Calamari EL, Camacho DM, Fadel CW, *et al*. A complex human gut microbiome cultured in an anaerobic intestine-on-a-chip. *Nat Biomed Eng* 2019;3:520–531.
30. Moossavi S, Arrieta M-C, Sanati-Nezhad A, Bishehsari F. Gut-on-chip for ecological and causal human gut microbiome research. *Trends Microbiol* 2022;30:710–721.
31. Scarpellini E, Ianiro G, Attili F, Bassanelli C, De Santis A, *et al*. The human gut microbiota and virome: potential therapeutic implications. *Dig Liver Dis* 2015;47:1007–1012.
32. Gacesa R, Kurilshikov A, Vich Vila A, Sinha T, Klaassen MAY, *et al*. Environmental factors shaping the gut microbiome in a Dutch population. *Nature* 2022;604:732–739.
33. Bajinka O, Tan Y, Abdelhalim KA, Özdemir G, Qiu X. Extrinsic factors influencing gut microbes, the immediate consequences and restoring eubiosis. *AMB Express* 2020;10:130.
34. García-Gutiérrez E, Almendros C, Mojica FJM, Guzmán NM, García-Martínez J. CRISPR content correlates with the pathogenic potential of *Escherichia coli*. *PLoS One* 2015;10:e0131935.
35. Zaura E, Brandt BW, Teixeira de Mattos MJ, Buijs MJ, Caspers MPM, *et al*. Same exposure but two radically different responses to antibiotics: resilience of the salivary microbiome versus long-term microbial shifts in feces. *mBio* 2015;6:e01693–15.
36. Konstantinidis T, Tsigalou C, Karvelas A, Stavropoulou E, Voidarou C, *et al*. Effects of antibiotics upon the gut microbiome: a review of the literature. *Biomedicines* 2020;8:8.
37. Kappel BA, De Angelis L, Heiser M, Ballanti M, Stoehr R, *et al*. Cross-omics analysis revealed gut microbiome-related metabolic pathways underlying atherosclerosis development after antibiotics treatment. *Mol Metab* 2020;36:100976.
38. Anthony WE, Wang B, Sukhum KV, D'Souza AW, Hink T, *et al*. Acute and persistent effects of commonly used antibiotics on the gut microbiome and resistome in healthy adults. *Cell Rep* 2022;39:110649.
39. d'Hérelle F. Sur un microbe invisible antagoniste des bacilles dysentériques. *CR Acad Sci Paris* 1917;165:373–375.
40. Abedon ST, Kuhl SJ, Blasdel BG, Kutter EM. Phage treatment of human infections. *Bacteriophage* 2011;1:66–85.
41. Rodriguez JM, Woodworth BA, Horne BA, Fackler J, Brownstein MJ. Case report: successful use of phage therapy in refractory MRSA chronic rhinosinusitis. *Int J Infect Dis* 2022;121:14–16.
42. Kuipers S, Ruth MM, Mientjes M, de Sévaux RGL, van Ingen J. A Dutch case report of successful treatment of chronic relapsing urinary tract infection with bacteriophages in a renal transplant patient. *Antimicrob Agents Chemother* 2019;64:01281–19.
43. Bao J, Wu N, Zeng Y, Chen L, Li L, *et al*. Non-active antibiotic and bacteriophage synergism to successfully treat recurrent urinary tract infection caused by extensively drug-resistant *Klebsiella pneumoniae*. *Emerg Microbes Infect*20209771774
44. Leitner L, Ujmajuridze A, Chanishvili N, Goderdzishvili M, Chkonia I, *et al*. Intravesical bacteriophages for treating urinary tract infections in patients undergoing transurethral resection of the prostate: a randomised, placebo-controlled, double-blind clinical trial. *Lancet Infect Dis* 2021;21:427–436.
45. Lebeaux D, Merabishvili M, Caudron E, Lannoy D, Van Simaey L, *et al*. A case of phage therapy against pandrug-resistant *Achromobacter xylosoxidans* in a 12-year-old lung-transplanted cystic fibrosis patient. *Viruses* 2021;13:60.
46. Wu N, Dai J, Guo M, Li J, Zhou X, *et al*. Pre-optimized phage therapy on secondary *Acinetobacter baumannii* infection in four critical COVID-19 patients. *Emerg Microbes Infect* 2021;10:612–618.
47. Nick JA, Dedrick RM, Gray AL, Vladar EK, Smith BE, *et al*. Host and pathogen response to bacteriophage engineered against *Mycobacterium abscessus* lung infection. *Cell* 2022;185:1860–1874.
48. Rao S, Betancourt-Garcia M, Kare-Opaneye YO, Swierczewski BE, Bennett JW, *et al*. Critically ill patient with multidrug-resistant *Acinetobacter baumannii* respiratory infection successfully treated with intravenous and nebulized bacteriophage therapy. *Antimicrob Agents Chemother* 2022;66:e0082421.
49. Petrovic Fabijan A, Lin RCY, Ho J, Maddocks S, Ben Zakour NL, *et al*. Safety of bacteriophage therapy in severe *Staphylococcus aureus* infection. *Nat Microbiol* 2020;5:465–472.
50. Simner PJ, Cherian J, Suh GA, Bergman Y, Beisken S, *et al*. Combination of phage therapy and cefiderocol to successfully treat *Pseudomonas aeruginosa* cranial osteomyelitis. *JAC Antimicrob Resist* 2022;4:dlac046.
51. Eskenazi A, Lood C, Wubbolts J, Hites M, Balarjishvili N, *et al*. Combination of pre-adapted bacteriophage therapy and antibiotics for treatment of fracture-related infection due to pandrug-resistant *Klebsiella pneumoniae*. *Nat Commun* 2022;13:302.
52. Pinto G, Shetty SA, Zoetendal EG, Gonçalves RFS, Pinheiro AC, *et al*. An *in vitro* fermentation model to study the impact of bacteriophages targeting Shiga toxin-encoding *Escherichia coli* on the colonic microbiota. *NPJ Biofilms Microbiomes* 2022;8:74.

53. Nale JY, Redgwell TA, Millard A, Clokie MRJ. Efficacy of an optimised bacteriophage cocktail to clear *Clostridium difficile* in a batch fermentation model. *Antibiotics* 2018;7:13.
54. Cieplak T, Soffer N, Sulakvelidze A, Nielsen DS. A bacteriophage cocktail targeting *Escherichia coli* reduces *E. coli* in simulated gut conditions, while preserving a non-targeted representative commensal normal microbiota. *Gut Microbes* 2018;9:391–399.
55. Jakobsen RR, Trinh JT, Bomholtz L, Brok-Lauridsen SK, Sulakvelidze A, *et al*. A bacteriophage cocktail significantly reduces *Listeria monocytogenes* without deleterious impact on the commensal gut microbiota under simulated gastrointestinal conditions. *Viruses* 2022;14:190.
56. Laforêt F, Antoine C, Lebrun S, Gonza I, Goya-Jorge E, *et al*. Impact assessment of vB_KpnP_K1-ULIP33 bacteriophage on the human gut microbiota using a dynamic *in vitro* model. *Viruses* 2023;15:719.
57. Moye ZD, Woolston J, Abbeele PV den, Duysburgh C, Verstrepen L, *et al*. A bacteriophage cocktail eliminates *Salmonella Typhimurium* from the human colonic microbiome while preserving cytokine signaling and preventing attachment to and invasion of human cells by *Salmonella in vitro*. *J Food Prot* 2019;82:1336–1349.
58. Kutateladze M, Adamia R. Phage therapy experience at the Eliava Institute. *Med Mal Infect* 2008;38:426–430.
59. Międzybrodzki R, Hoyle N, Zhvaniya F, Łusiak-Szelachowska M, Weber-Dąbrowska B, *et al*. Current updates from the long-standing phage research centers in Georgia, Poland, and Russia. In: *Bacteriophages: Biology, Technology, Therapy*. 2021. pp. 921–951.
60. Corbellino M, Kieffer N, Kutateladze M, Balarjishvili N, Leshkasheli L, *et al*. Eradication of a multidrug-resistant, carbapenemase-producing *Klebsiella pneumoniae* isolate following oral and intra-rectal therapy with a custom-made, lytic bacteriophage preparation. *Clin Infect Dis* 2020;70:1998–2001.
61. Zschach H, Joensen KG, Lindhard B, Lund O, Goderdzishvili M, *et al*. What can we learn from a metagenomic analysis of a Georgian bacteriophage cocktail? *Viruses* 2015;7:6570–6589.
62. Chen S, Zhou Y, Chen Y, Gu J. fastp: an ultra-fast all-in-one FASTQ preprocessor. *Bioinformatics* 2018;34:i884–i890.
63. Beghini F, McIver LJ, Blanco-Míguez A, Dubois L, Asnicar F, *et al*. Integrating taxonomic, functional, and strain-level profiling of diverse microbial communities with bioBakery 3. *eLife* 2021;10:e65088.
64. Wood DE, Lu J, Langmead B. Improved metagenomic analysis with Kraken 2. *Genome Biol* 2019;20:257.
65. Lu J, Breitwieser FP, Thielen P, Salzberg SL. Bracken: estimating species abundance in metagenomics data. *PeerJ Comput Sci* 2017;3:e104.
66. Kleverov M, Zenkova D, Kamenev V, Sablina M, Artyomov MN, *et al*. Phantasus: web-application for visual and interactive gene expression analysis. *Bioinformatics* 2022;2022:2022.
67. Dixon P. VEGAN, a package of R functions for community ecology. *J Veg Sci* 2003;14:927–930.
68. Li D, Liu C-M, Luo R, Sadakane K, Lam T-W. MEGAHIT: an ultra-fast single-node solution for large and complex metagenomics assembly via succinct *de Bruijn* graph. *Bioinformatics* 2015;31:1674–1676.
69. Telatin A, Fariselli P, Birolo G. SeqFu: a suite of utilities for the robust and reproducible manipulation of sequence files. *Bioengineering* 2021;8:59.
70. Eren AM, Esen ÖC, Quince C, Vineis JH, Morrison HG, *et al*. Anvi'o: an advanced analysis and visualization platform for 'omics data. *PeerJ* 2015;3:e1319.
71. Eren AM, Kiefl E, Shaiber A, Veseli I, Miller SE, *et al*. Community-led, integrated, reproducible multi-omics with anvi'o. *Nat Microbiol* 2021;6:3–6.
72. Li W, Godzik A. Cd-hit: a fast program for clustering and comparing large sets of protein or nucleotide sequences. *Bioinformatics* 2006;22:1658–1659.
73. Nayfach S, Camargo AP, Schulz F, Eloe-Fadrosh E, Roux S, *et al*. CheckV assesses the quality and completeness of metagenome-assembled viral genomes. *Nat Biotechnol* 2021;39:578–585.
74. Turner D, Kropinski AM, Adriaenssens EM. A roadmap for genome-based phage taxonomy. *Viruses* 2021;13:506.
75. Langmead B, Salzberg SL. Fast gapped-read alignment with Bowtie 2. *Nat Methods* 2012;9:357–359.
76. Li H, Handsaker B, Wysoker A, Fennell T, Ruan J, *et al*. The Sequence Alignment/Map format and SAMtools. *Bioinformatics* 2009;25:2078–2079.
77. Tatusov RL, Galperin MY, Natale DA, Koonin EV. The COG database: a tool for genome-scale analysis of protein functions and evolution. *Nucleic Acids Res* 2000;28:33–36.
78. Chan PP, Lowe TM. tRNAscan-SE: searching for tRNA genes in genomic sequences. *Methods Mol Biol* 2019;1962:1–14.
79. Bin Jang H, Bolduc B, Zablocki O, Kuhn JH, Roux S, *et al*. Taxonomic assignment of uncultivated prokaryotic virus genomes is enabled by gene-sharing networks. *Nat Biotechnol* 2019;37:632–639.
80. Cook R, Brown N, Redgwell T, Rihtman B, Barnes M, *et al*. INfrastructure for a PHAge REference database: identification of large-scale biases in the current collection of cultured phage genomes. *Phage* 2021;2:214–223.
81. Bouras G, Nepal R, Houtak G, Psaltis AJ, Wormald P-J, *et al*. Pharokka: a fast scalable bacteriophage annotation tool. *Bioinformatics* 2023;39:39.
82. Buchfink B, Xie C, Huson DH. Fast and sensitive protein alignment using DIAMOND. *Nat Methods* 2015;12:59–60.
83. Nepusz T, Yu H, Paccanaro A. Detecting overlapping protein complexes in protein-protein interaction networks. *Nat Methods* 2012;9:471–472.
84. Shannon P, Markiel A, Ozier O, Baliga NS, Wang JT, *et al*. Cytoscape: a software environment for integrated models of biomolecular interaction networks. *Genome Res* 2003;13:2498–2504.
85. Gilchrist CLM, Chooi YH. Clinker & clustermap.js: automatic generation of gene cluster comparison figures. *Bioinformatics* 2021;37:2473–2475.
86. Thorvaldsdóttir H, Robinson JT, Mesirov JP. Integrative Genomics Viewer (IGV): high-performance genomics data visualization and exploration. *Brief Bioinform* 2013;14:178–192.
87. Birolo G, Telatin A. BamToCov: an efficient toolkit for sequence coverage calculations. *Bioinformatics* 2022;38:2617–2618.
88. Roux S, Camargo AP, Coutinho FH, Dabdoub SM, Dutilh BE, *et al*. iPHoP: an integrated machine learning framework to maximize host prediction for metagenome-derived viruses of archaea and bacteria. *PLoS Biol* 2023;21:e3002083.
89. Hockenberry AJ, Wilke CO. BACPHLIP: predicting bacteriophage lifestyle from conserved protein domains. *PeerJ* 2021;9:e11396.
90. Kieft K, Anantharaman K. Deciphering active prophages from metagenomes. *mSystems* 2022;7:e00084–22.
91. Roux S, Adriaenssens EM, Dutilh BE, Koonin EV, Kropinski AM, *et al*. Minimum Information about an Uncultivated Virus Genome (MIUViG). *Nat Biotechnol* 2019;37:29–37.
92. Lopez-Diaz M, Bleriot I, Pacios O, Fernandez-Garcia L, Blasco L, *et al*. Molecular characteristics of phages located in carbapenemase-producing *Escherichia coli* clinical isolates: new phage-like plasmids. *Bioinformatics*;2022:29. DOI: 10.1101/2022.06.29.498070.
93. Fassarella M, Blaak EE, Penders J, Nauta A, Smidt H, *et al*. Gut microbiome stability and resilience: elucidating the response to perturbations in order to modulate gut health. *Gut* 2021;70:595–605.